

https://doi.org/10.1070/QEL17423

Effect of CO_2-laser power density on the absorption coefficient of polycrystalline CVD diamonds

M.S. Andreeva, N.V. Artyushkin, M.I. Krymskii, A.I. Laptev, N.I. Polushin, V.E. Rogalin, M.V. Rogozhin

Abstract. **The effect of 1-s irradiation of an uncooled polycrystalline CVD diamond plate by a focused cw CO_2 laser beam with a power density of 300–800 kW cm^{-2} is investigated. The absorption coefficient of the sample at a power density of 800 kW cm^{-2} is found to be 0.035 cm^{-1} larger as compared with that at 300 kW cm^{-2}, which is related to the temperature dependence of its phonon-induced absorption with a change in temperature from 44 to 100 °C. It is shown that polycrystalline diamond, in contrast to other optical materials, does not exhibit nonlinear (avalanche-like) rise in absorption at high CO_2-laser power densities, at least up to 800 kW cm^{-2}.**

Keywords: *polycrystalline CVD diamond, CO_2 laser, radiation, power density, absorption coefficient, output window, pyrometer, mathematical simulation.*

1. Introduction

After publication [1], where unique radiation resistance of diamond exposed to a focused beam of 10-kW cw CO_2 laser was demonstrated for the first time, the potential of diamond as a material for laser optical elements (in particular, gas-laser output windows) has been intensively studied.

Many IR devices operate in the atmospheric transparency window of 8–14 μm. Among them, CO_2 lasers with a working wavelength of 10.6 μm are considered as the most important ones. To date, lasers with power up to 1 MW in the cw and repetitively pulsed regimes and energy of several tens of kilojoules in the pulsed regime have been developed [2]. One of the most vulnerable units of a laser is its output window [3]. To extract radiation from the gas cell into atmosphere, it was necessary to search for appropriate optical materials, because conventional materials (glasses transparent in visible light) are opaque in the 10-μm spectral region. Eventually, diamond was accepted to be the most promising material for high-power CO_2 lasers [1]. However, it took many years to obtain diamond plates that could be used in practice as laser output windows. Additionally, some related problems have been solved: optical processing of diamonds [4–6] and deposition of interference coatings on diamond articles [7].

Due to the development of CVD diamond technology [8], diamond has started being incorporated very rapidly into various high-tech products [6, 9–16]. The point is that this material has a unique combination of physicochemical properties. In particular, it possesses the highest thermal conductivity (exceeding that of copper by a factor of 5) and hardness; it has also high chemical and radiation resistance and is transparent in a wide spectral range (from the UV range to the centimetre wavelength range, except for the phonon absorption range from 2 to 6 μm). Diamond has a fairly low (0.8×10^{-6} K^{-1} at $T = 273$ K) coefficient of thermal expansion (CTE), which can be compared with that of Invar but is much lower than the CTE of traditionally used optical materials. It has also some other remarkable properties [6, 12, 16, 17]. The CVD process provides technologically reproducible plates of polycrystalline diamond (PCD) of optical quality up to 200 mm in diameter and several millimetres thick [6, 12]. For example, output windows 100 mm in diameter (and somewhat larger in some cases) for megawatt millimetre-range gyrotrons are made of only CVD diamonds [18, 19]. Diamond windows are also applied in THz lasers [20].

The absorption coefficients α of single-crystal and polycrystalline diamonds in the vicinity of 10.6 μm are some different and, depending on the quality of material, range from 0.03 to 0.065 cm^{-1} [9, 16, 21]. Two-phonon lattice absorption is known to dominate in diamond in the vicinity of 10 μm [22]; this circumstance does not allow one to obtain a material with $\alpha \leqslant 0.03$ cm^{-1}. This value greatly exceeds the corresponding characteristics of the main competitors of diamond, ZnSe and KCl, which have $\alpha \sim 10^{-4}$ cm^{-1}. Nevertheless, due to its much better mechanical and thermophysical properties, diamond turned out to be much ahead of its competitors [9, 23].

Although single-crystal diamonds have lower absorption than PCDs, specifically the latter are used as a material of laser windows, because the sizes of commercial diamond single crystals generally rarely exceed 10 mm, which is too small for the size of output window, which should also be vacuumised, fastened, and connected with a cooling system. In this context, we should mention the recent technical solution [24, 25] combining the advantages of single-crystal and polycrystalline diamonds: a single-crystal insert is grown in a PCD plate, through which most of the laser beam is transmitted, whereas most of construction load is distributed over the polycrystalline part of the window.

When high-power CO_2 slit lasers with compact high-intensity beams were developed, the use of diamond optics became obligatory, despite its high cost [9, 16, 26].

M.S. Andreeva Lomonosov Moscow State University, Vorob'evy gory, 119991 Moscow, Russia;
N.V. Artyushkin, M.I. Krymskii, A.I. Laptev, N.I. Polushin, M.V. Rogozhin National University of Science and Technology MISiS, Leninsky prosp. 4, 119049 Moscow, Russia;
V.E. Rogalin Institute for Electrophysics and Electric Power, Russian Academy of Sciences, Dvortsovaya nab. 18, 191186 St. Petersburg, Russia; e-mail: v-rogalin@mail.ru

Received 18 August 2020; revision received 5 October 2020
Kvantovaya Elektronika **50** (12) 1140–1145 (2020)
Translated by Yu.P. Sin'kov

One of important applications of high-power CO_2 lasers is relatively new; it is the use of laser-generated plasma as a source of intense radiation in projection X-ray photolithography in order to fabricate integrated circuits of diminished sizes [13–15]. To use this system with a high efficiency, one needs a CO_2 laser stably operating in a technological production line, and its output power should be continuously maintained at a level of several tens of kilowatts in correspondence with specified operation regime. In this case, the most important component of CO_2 laser is its cooled diamond output window.

Thus, the operation of laser windows transmitting intense cw laser beams with power densities of several tens of kW cm^{-2} must be stable. In the case of repetitively pulsed regime, the specific load on a diamond window increases to several hundreds of kW cm^{-2} or even more, which is two orders of magnitude higher than the intensity the diamond competitors can withstand [27]. The optical and thermomechanical processes occurring in the output window of a high-power laser were considered in [28, 29]. However, that consideration disregarded the fact that diamond is a wide-gap semiconductor, in which various nonlinear effects in high-power electromagnetic fields (related to the ionisation of impurity levels) may manifest themselves. Therefore, under such high radiation loads, the absorption coefficient may increase not only due to thermophysical effects but also for some other reasons.

The temperature dependence of the diamond absorption coefficient at a wavelength of 10.6 μm in the range of 20–500 °C was measured by laser calorimetry in [30]. Two samples with absorption coefficients $\alpha = 0.096$ and 0.85 cm^{-1} were investigated at room temperature. The temperature dependences $\alpha(T)$ were identical in both cases: the coefficient α increased by about 0.5 cm^{-1} with an increase in temperature to 500 °C. Similar data were obtained in [31, 32], where the temperature dependences of absorption in diamond were analysed. However, in all these studies laser calorimetry was performed with low-power radiation sources, and the sample temperature was increased using an external heater.

In this study we investigated the change in the absorption coefficient of polycrystalline CVD diamond exposed to only a CO_2 laser beam in the range of power densities from 300 to 800 kW cm^{-2} in order to determine the influence of the 10.6-μm radiation intensity on the diamond absorption. The sample was heated as a result of the absorption of laser beam transmitted through it.

2. Experimental

The objects of study were optically polished plane-parallel polycrystalline CVD diamond plates 10 mm in diameter and 0.5 mm thick. The sample surface roughness R_{ms} was estimated from measurements on a scanning probe microscope MFP 3D Stand Alone (Asylum Research) using a silicon cantilever at a resonance frequency of 120 kHz and the program Gwyddion (version 2.51); it turned out to be 1.36 nm.

The radiation source was a technological laser TL-1.5 with an output power up to 1.5 kW in the cw regime and a beam divergence of 3×10^{-3} rad. The output-beam diameter was 20 mm. The laser power could be deliberately changed in the range from 0.050 to 1.5 kW. The radiation power was measured using a standard meter with indication on the control console. The laser in use was equipped (specially for this experiment) with a locking circuit, which made it possible to open the shutter at the laser output for 0.3–1.0 s. It was necessary to limit the irradiation time in order to exclude the influence of extra sample heating on the measured characteristics.

A schematic of the experiment is shown in Fig. 1. The laser beam was focused on the sample by a single-lens objective made of a potassium chloride (KCl) single crystal 40 mm in diameter with a focal length of 90 mm. A polycrystalline diamond sample in a Teflon mounting was installed in the focal region of the single-lens objective.

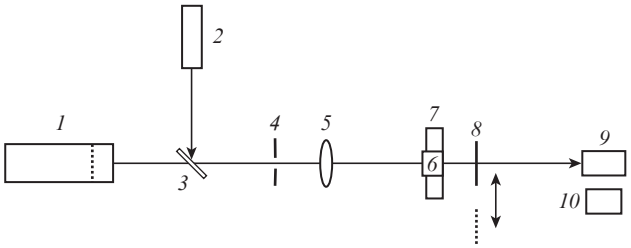

Figure 1. Schematic of the experiment:
(*1*) TL-1.5 laser with external shutter; (*2*) adjusting laser; (*3*) plate for aligning laser beams; (*4*) diaphragm; (*5*) single-lens objective; (*6*) sample; (*7*) mounting; (*8*) metal screen; (*9*) TM-908 pyrometer; (*10*) stop watch.

Lasing was performed with a successive increase in the output power from 200 to 700 W with a step of 100 W; the irradiation time was 1 s. After switching off the laser, the protective 5-mm-thick steel screen was removed from the optical scheme, and the sample temperature was measured by a TM-908 pyrometer. The pyrometer head was located at a distance of 5 cm from the sample. Although the radiation power density in our experiment was much lower than that in [33, 34], cooling was absent; therefore, the laser power was not further increased to avoid irreversible sample damage.

3. Results and discussion

The polycrystalline diamond sample under study had relatively small sizes. At the same time, to perform optical measurements of the plate temperature, it was necessary to locate the detector head maximally close to the sample. Therefore, we used a pyrometer rather than an infrared imager, which was applied in [34].

Based on the results of each laser shot, we plotted a dependence of the sample temperature on the cooling time after the end of laser irradiation and protective screen removal (about 1 s after the end of irradiation). The character of the sample cooling curves at different radiation power densities can be seen in Fig. 2.

The average sample temperature was recorded by a TM-908 pyrometer 1 s after switching off the laser. At the same time, to calculate correctly the absorption coefficient based on the experimental data obtained, one must know the sample temperature in the objective focal region directly at the end of laser irradiation. Therefore, to correct the temperature data, the curves showing the change in the temperature after irradiation (see Fig. 2) were extrapolated to 1 s (the time between the instant of switching off the laser and the pyrometer operation onset). The calculations were performed below using the extrapolated temperature values T_{extr}.

Figure 3 shows the dependences (plotted based on the data obtained) of the maximum relative temperature of the

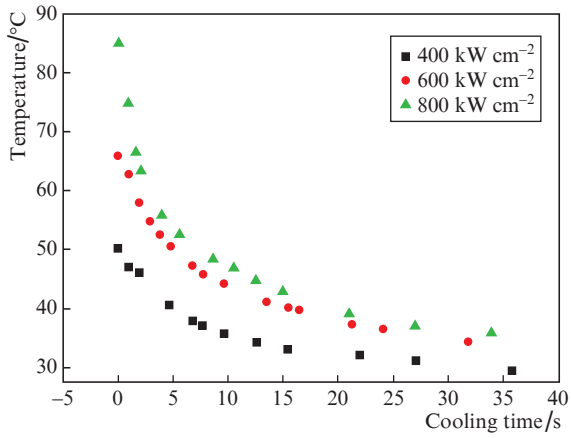

Figure 2. Dependences of the sample temperature on the cooling time at laser power densities of 400, 600, and 800 kW cm^{-2}. The laser irradiation time is 1 s.

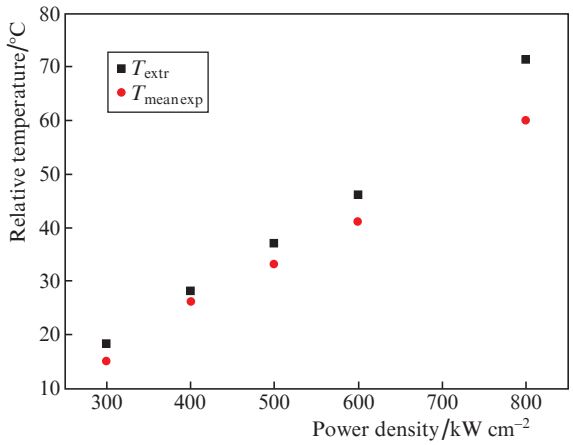

Figure 3. Dependences of the maximum relative sample temperature $T_{mean\,exp}$ in the focal region, recorded by pyrometer, and the extrapolated temperature T_{extr} on the laser power density.

sample [the difference between the absolute temperature recorded by the pyrometer 1 s after switching off the laser, $T_{mean\,exp}$, and the background temperature (25 °C)] and the extrapolated temperature T_{extr} on the radiation power density.

To carry out a preliminary analysis of the radial temperature distribution over the sample (in order to calculate its mean value) and subsequent calculation of the absorption coefficient based on experimental results, we used the mathematical model of a cw-laser output window [28] in the part concerning the calculation of its temperature field during operation.

The following heat conduction equation in cylindrical coordinates was solved numerically using the locally one-dimensional Samarskii scheme [35] (which is absolutely stable and possesses the property of total approximation):

$$\rho c\frac{\partial T}{\partial t} = \frac{1}{r}\frac{\partial}{\partial r}\left(\lambda r\frac{\partial T}{\partial r}\right) + Q(r,z). \qquad (1)$$

Here, ρ is density; λ is thermal conductivity; c is specific heat; r is the radius of the plate in question; and $Q(r,z)$ is the absorbed radiation power density, which is determined for a Gaussian profile as

$$Q(r,z) = 2\frac{P_0\alpha}{\pi W_0^2}\exp\left(-2\frac{r^2}{W_0^2}\right), \qquad (2)$$

where P_0 is the laser power, α is the absorption coefficient at the laser wavelength, and W_0 is the irradiated spot radius. The model takes into account the temperature dependence of the thermal conductivity λ of the window material. For the temperature range considered here (300–600 K), the dependences $\lambda \sim f(T)$ can be approximated well by the formula

$$\lambda(T) = \lambda_0\frac{T_0}{T}, \qquad (3)$$

where λ_0 is the thermal conductivity at the initial temperature T_0 (the calculations were performed with T_0 = 300 K).

The following adiabatic boundary condition on the window symmetry axis was imposed:

$$r = 0, \quad \lambda\partial T/\partial r = 0. \qquad (4)$$

The calculation was performed in the Gaussian beam approximation with the following parameters for diamond [36, 37]: thermal conductivity (at T = 300 K) 2000 W m^{-1} K^{-1}, specific heat 520 J kg^{-1} K^{-1}, and density 3515 kg m^{-3}.

The above-reported parameters of the PCD plate and laser beam in the objective focus were used as the input values for the calculation model. Since the pyrometer measured the averaged temperature value T_{mean} in the region of window light diameter and the beam spot size in the objective focus was much smaller than this diameter, the temperature T in the focal region was calculated numerically.

The model in use does not take into account the heat losses into the sample holder and the atmosphere during the first second of the laser irradiation, but it allows one to estimate the heat distribution rate in the diamond plate and the temperature equalisation over its area. At this instant the main heat loss from the irradiated region occurs as a result of heat flow redistribution in the diamond. The heat loss into the environment can be neglected, because the spot sizes are small and the thermal conductivity of air negligible in comparison with that of diamond. The heat flow arriving at the sample mounting is significantly attenuated; therefore, we neglected it as well.

In the cooling stage heat is transferred from the diamond to the mounting and environment. The heat loss is small in view of the small difference in temperatures; therefore, the final stage of sample cooling is relatively long. Specifically its duration determines the final heat loss of the sample.

To perform a comparative analysis of the maximum (in the laser-irradiated region) and sample-averaged temperatures using the developed model, we calculated the radial temperature distribution over the sample at the switching-off instant with different laser power densities I. The calculation results are presented in Figs 4 and 5.

Figure 4 shows three-dimensional distributions of the temperature difference $\Delta T = T - T_{mean}$ at an irradiation time of 1 s and the following laser power densities on the sample surface: I = 300, 500, and 800 kW cm^{-2}.

Figure 5 presents the radial distributions of $\Delta T = T - T_{mean}$ at different I values; one can see that the temperatures T and T_{mean} are rather close in view of the high thermal conductivity of diamond.

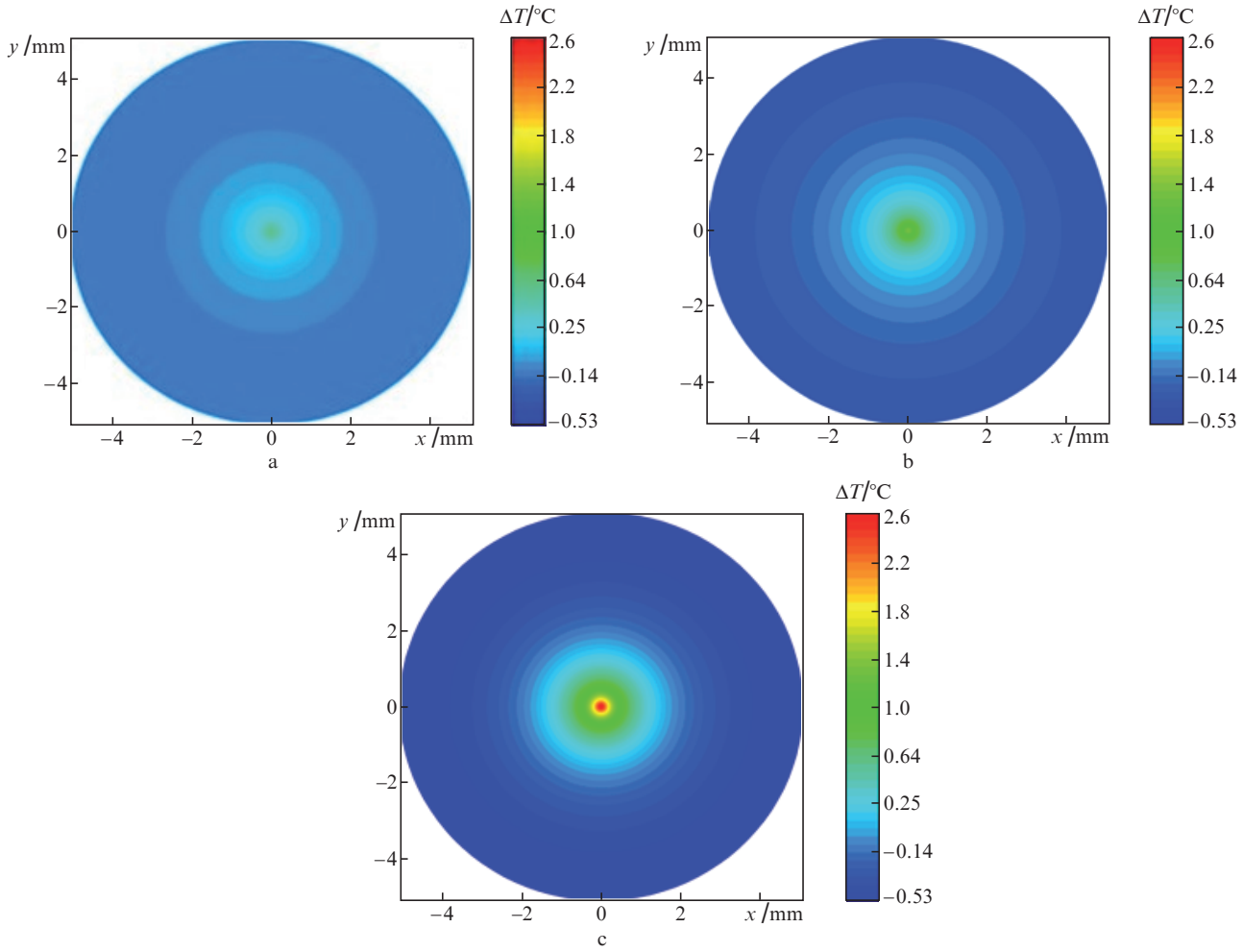

Figure 4. Distributions of temperature difference $\Delta T = T - T_{mean}$ in the sample at the instant of switching off the laser for I = (a) 300, (b) 500, and (c) 800 kW cm^{-2}.

As follows from the data of Figs 4 and 5, the difference between the sample-averaged temperature T_{mean} and the maximum (in the focal region with an area of ~0.07 mm^2) temperature T in the PCD sample is small; hence, the error in the experimental results due to insufficiently high pyrometer resolution is insignificant. Therefore, when calculating the absorption coefficient of the sample, one can use the value of measured averaged temperature extrapolated to the instant of switching off the laser, T_{extr} (see Fig. 3).

Note that the numerically calculated temperature distributions in Figs 4 and 5 have a qualitative character, because the calculation was performed disregarding the temperature dynamics of the diamond absorption coefficient during 1-s laser heating. The main purpose of these calculations was to determine the validity of the averaged temperature values measured by the pyrometer.

Then the program performed numerical fitting of the absorption coefficient α applied at the calculation model input so as to make the calculated temperature value coincide with the extrapolated value T_{extr} of pyrometer-measured temperature for a laser irradiation time of 1 s.

Table 1 contains calculated values of PCD absorption coefficient at a wavelength of 10.6 μm in the range of laser power densities from 300 to 800 kW cm^{-2}. It follows from these data that the absorption coefficient increases by 0.035 cm^{-1} with an increase in I from 300 to 800 kW cm^{-2}.

Table 1. Absorption coefficient of polycrystalline CVD diamond at a wavelength of 10.6 μm for different laser power densities.

α (cm^{-1})	I (W/cm^2)	$T_{mean\,exp}$ (°C)	T_{extr} (°C)	T (°C)
0.12	3×10^5	40.0	43.3	44.2
0.132	4×10^5	50.2	53.4	54.7
0.137	5×10^5	58.0	62.5	63.9
0.148	7×10^5	65.9	70.9	72.8
0.155	8×10^5	85.1	96.4	100

Note: Temperature $T_{mean\,exp}$ was measured approximately 1 s after the removal of protective screen; the temperatures directly after switching off the laser (T_{extr}) were obtained by extrapolating the dependences $T_{mean\,exp}$ (t) to the instant of switching off the laser, and the T values were obtained from calculations.

Figure 6 shows a dependence of the absorption coefficient of the PCD sample on the power density in the region irradiated by CO_2 laser.

In our case we observed the same tendency of rise in the absorption coefficient with temperature as in [29–31]. In particular, it was found in [30] that the absorption coefficient of diamond increased by 0.05 cm^{-1} upon external heating in the same temperature range. We believe that the rise in the PCD absorption coefficient with an increase in the CO_2-laser power density, which was observed in our experiments, is also caused by the temperature-dependent phonon-induced absorption

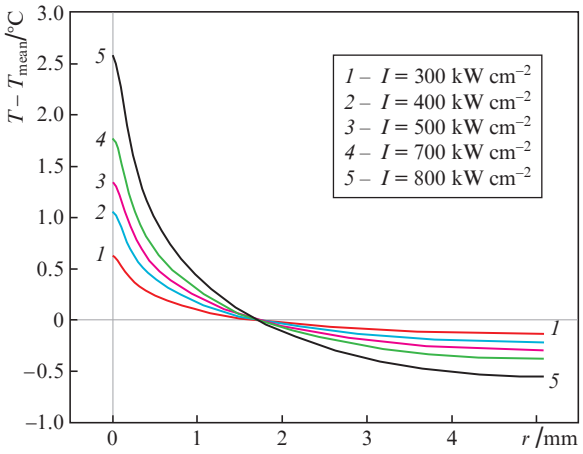

Figure 5. Radial dependences of the temperature difference $T - T_{mean}$ at the end of laser irradiation.

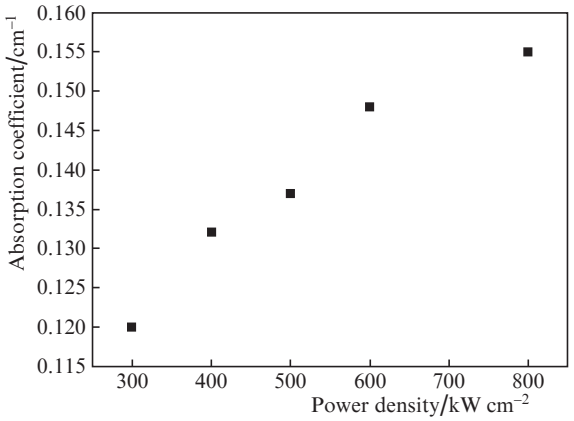

Figure 6. Dependence of the sample absorption coefficient on the power density in the region irradiated by CO_2 laser.

rather than the temperature-independent impurity mechanism. As the experiment showed, PCD does not exhibit nonlinear (avalanche-like) rise in absorption at CO_2 laser power densities at least up to 800 kW cm^{-2}, which greatly exceeds the limit for other similar-purpose materials [27]. We did not exceed the level of 800 kW cm^{-2} because this value is much larger than the power densities in the laser systems used in practice.

4. Conclusions

The effect of 1-s irradiation of an uncooled polycrystalline CVD-diamond plate by a focused cw laser beam in the range of power densities from 300 to 800 kW cm^{-2} was investigated. The PCD absorption coefficient was found to increase by 0.035 cm^{-1} with an increase in the laser power density to 800 kW cm^{-2}. This result is consistent with the data of [30], where transmission of a weak beam through a sample upon external heating in the same temperature range (44–100 °C) as in our study was analysed. Based on this, we suggest the observed rise in the absorption coefficient with an increase CO_2 laser power density to be also caused by the temperature-dependent phonon-induced absorption. It was shown that PCD, in contrast to other optical materials, does not exhibit any nonlinear (avalanche-like) rise in absorption at CO_2 laser power densities at least up to 800 kW cm^{-2}; therefore, the optical elements made of polycrystalline diamond can operate at ultrahigh light power densities.

Acknowledgements. The PCD optical properties were measured at the interdepartment educational and training laboratory of semiconductor materials and insulators "Single Crystals and Preforms Based on Them" at the National University of Science and Technology MISiS.

This study was performed within a federal target project of the programme 'Investigation and Engineering in High-Priority Lines of Development of Science and Technology in Russia for 2014–2020,' the subject 'Development of the Technology and Equipment for Growing Ultrapure Diamond Single Crystals by the CVD Method and Doping Them for Use in Photonics and Microelectronics As High-Temperature Semiconductors' within an agreement for Grant No. 075-02-2018-210 on November 26, 2018 (unique identifier of the convention RFMEFI57818X0266), with support of applied research by the Ministry of Education and Science of the Russian Federation.

References

1. Douglas-Hamilton D., Hoad E.D., Seitz J.R.M. *J. Opt. Soc. Am.*, **64**, 36 (1974).
2. Baranov G.A., Kuchinskii A.A. *Quantum Electron.*, **35**, 219 (2005) [*Kvantovaya Elektron.*, **35**, 219 (2005)].
3. Shmakov V.A. *Silovaya optika* (Power Optics) (Moscow: Nauka, 2004).
4. Pickles C.S.J., Madgwick T.D., Sussmann R.S., Wort C.J.H. *Diam. Relat. Mater.*, **9**, 916 (2000).
5. Balmer R.S., Brandon J.R., Clewes S.L., Dhillon H.K., Dodson J.M., Friel I., Inglis P.N., Madgwick T.D., Markham M.L., Mollart T.P., Perkins N., Scarsbrook G.A., Twitchen D.J., Whitehead A.J., Wilman J.J., Woollard S.M. *J. Phys. Condens. Matter.*, **21**, 364221 (2009).
6. Konov V.I. (Ed.) *Uglerodnaya fotonika* (Carbon Photonics) (Moscow: Nauka, 2017).
7. Pivovarov P.A., Pavel'ev V.S., Soifer V.A., Cherepanov K.V., Anisimov V.I., Butuzov V.V., Sorochenko V.R., Artyushkin N.V., Rogalin V.E., Shchebetova N.I., Plotnichenko V.G., Konov V.I. *Quantum Electron.*, **48**, 1000 (2018) [*Kvantovaya Elektron.*, **48**, 1000 (2018)]; https://doi.org/10.1070/QEL16855.
8. Spitsyn B.V., Deryagin B.V. USSR Inventor's Certificate No. 339134 (priority date 10 Yuly, 1956); *Byull. Izobret.*, No. 17, p. 233 (1980).
9. Sussman R.S., Brandon J.R., Coe S.E., Pickles C.S.J., Sweeney C.G., Wasenczuk A., Wort C.J.H., Dodge C.N.; www.e6.com.
10. Dodson J.M., Brandon J.R., Dhillon H.K., Friel I., Geoghegan S.L., Mollart T.P., Santini P., Scarsbrook G.A., Twitchen D.J., Whitehead A.J., Wilman J.J., de Wit H. *Proc. SPIE*, **8016**. 80160L (2011).
11. Anoikin E., Muhr A., Bennett An., Twitchen D.J., de Wit H. *Proc. SPIE*, **9346**, 93460T (2015).
12. Rogozhin M.V., Rogalin V.E., Krymskii M.I., Krymskii K.M. *J. Commun. Technol. Electron.*, **63**, 1326 (2018); DOI: 10.1134/S1064226918110098; [*Radiotekh. Elektron.*, **63**, 1188 (2018)]; DOI: 10.1134/S0033849418110098.
13. Endo A. http://www.intechopen.com; DOI: 10.5772/3871.
14. Nowak K.M., Ohta T., Suganuma T., Fujimoto J., Mizoguchi H., Sumitani A., Endo A. *Optoelectron. Rev.*, **21** (4), 345 (2013).
15. Aranchii S.M., Krymskii K.M., Krymskii M.I., Rogalin V.E. *J. Commun. Technol. Electron.*, **60**, 308 (2015); DOI: 10.1134/S1064226915030031 [*Radiotekh. Elektron.*, **60**, 325 (2015)]; DOI: 10.7868/S0033849415030031.
16. Rogalin V.E., Aranchii S.M. *Integral*, **5** (67), 80 (2012).
17. Ral'chenko V.G., Konov V.I. *Elektron. Nauka, Tekhnol., Bizness*, (4), 58 (2008).
18. Parshin V.V. *Int. J. Millimeter Waves*, **15**, 339 (1994).

19. Rogalin V.E., Kaplunov I.A., Kropotov G.I. *Opt. Spectrosc.*, **125**, 1053 (2018); DOI: 10.1134/S0030400X18120172; [*Opt. Spektrosk.*, **125**, 851 (2018)]; DOI: 10.21883/OS.2018.12.46951.190-18.
20. Vinokurov N.A., Shevchenko O.A. *Phys. Usp.*, **61**, 435 (2018) [*Usp. Fiz. Nauk*, **188**, 493 (2018)]; DOI: 10.3367/UFNr.2018.02.038311.
21. Luk'yanov A.Yu., Ral'chenko V.G., Khomich A.V., Serdtsev E.V., Volkov P.V., Savel'ev A.V., Konov V.I. *Quantum Electron.*, **38**, 1171 (2008) [*Kvantovaya Elektron.*, **38**, 1171 (2008)].
22. Mildren R.P., Rabeau J.R. (Eds) *Optical Engineering of Diamond* (Wiley-VCH Verlag GmbH & Co. KGaA, 2013).
23. Deutsch T.F. *J. Electron. Mater.*, **4**, 663 (1975).
24. Rogozhin M.V., Rogalin V.E., Krymskii M.I., Kaplunov I.A. *Diagn., Resour. Mech. Mater. Struct.*, (1), 34 (2018); DOI: 10.17804/2410-9908.2018.1.034-040.
25. Vikharev, A.L., Gorbachev A.M., Dukhnovskii M.P., Muchnikov A.B., Ratnikova A.K., Fedorov Yu.Yu. *Semiconductors*, **46**, 263 (2012); DOI: 10.1134/S1063782612020248 [*Fiz. Tekh. Poluprovodn.*, **46**, 274 (2012)].
26. Granson V., Sumrain Sh., Daniel P., Villarreal Fr., Deile J. *Proc. SPIE*, **6872**, 687209 (2008).
27. Loomis J.S., Huguley C.A. *NBS Spec. Publicat.*, **414**, 94 (1974).
28. Rogozhin M.V., Rogalin V.E., Krymskii M.I. *Opt. Spectrosc.*, **122** (5), 843 (2017); DOI: 10.1134/S0030400X17050186 [*Opt. Spektrosk.*, **122**, 873 (2017)]; DOI: 10.7868/S003040341705018X.
29. Rogozhin M.V., Rogalin V.E., Krymskii M.I., Filin S.A. *Bull. Russ. Acad. Sci.: Phys.*, **80**, 1260 (2016); DOI: 10.3103/ S1062873816100166; [*Izv. Akad. Nauk, Ser. Fiz.*, **80**, 1410 (2016)]; DOI: 10.7868/S0367676516100203.
30. Wörner E., Wild C., Müller-Sebert W., Grimm M., Koidl P. *Diamond Relat. Mater.*, **14**, 580 (2005).
31. Piccirillo C., Davies G., Mainwood A., Penchina C. *Phys. B Condens. Matter.*, **308–310**, 581 (2001).
32. Piccirillo C., Davies G., Mainwood A., Scarle S., Penchina C.M., Mollart T.P., Lewis K.L., Nesladek M., Remes Z., Pickles C.S.J. *J. Appl. Phys.*, **92** (2), 756 (2002).
33. Rogalin V.E., Ashkinazi E.E., Popovich A.F., Ral'chenko V.G., Konov V.I., Aranchii S.M., Ruzin M.V., Uspenskii S.A. *Izv. Vyssh. Uchebn. Zaved., Mater. Elektron. Tekh.*, (3), 41 (2011).
34. Rogalin V.E., Ashkinazi E.E., Popovich A.F., Ral'chenko V.G., Konov V.I., Aranchii S.M., Ruzin M.V., Rogozhin M.V. *Phys. Wave Phenom.*, **26**, 75 (2018); doi: 10.3103/S1541308X18020012.
35. Samarskii A.A. *Teoriya raznostnykh skhem* (Theory of Difference Schemes) (Moscow: Nauka, 1977).
36. Thomas M., Tropf W. *Johns Hopkins APL Techn. Digest*, **14**, 16 (1993).
37. The Element Six CVD Diamond Handbook; https://e6cvd.com/media/wysiwyg/pdf/E6_CVD_Diamond_Handbook_A5_v10X.pdf.